

Surface Modification of Polypropylene Microporous Membranes with a Novel Glycopolymer

Qian Yang,[†] Zhi-Kang Xu,^{*,†} Zheng-Wei Dai,[†] Jian-Li Wang,[‡] and Mathias Ulbricht[§]

Institute of Polymer Science, Zhejiang University, Hangzhou 310027, P. R. China, College of Chemical Engineering and Materials, Zhejiang University of Technology, Hangzhou 310014, P. R. China, and Institut für Technische Chemie, Universität Duisburg-Essen, 45117 Essen, Germany

Received November 12, 2004. Revised Manuscript Received February 12, 2005

Membrane-based biomedical processes have increased considerably in recent years. However, the natural disadvantages of common membrane materials, such as hydrophobic surface and poor biocompatibility, cause many side effects in use and hinder further applications. In this work, to meet the requirements of biomedical applications, a novel sugar-containing monomer (D-gluconamidoethyl methacrylate (GAMA)) was grafted on polypropylene microporous membrane (PPMM) with an UV-induced polymerization to improve both the surface hydrophilicity and hemocompatibility. Fourier transform infrared spectroscopy, X-ray photoelectron spectroscopy, and scanning electron microscopy were employed to confirm the surface modification on the membranes. Water contact angle, protein adsorption, and platelet adhesion measurements were used to evaluate the anti-fouling property and the hemocompatibility of the membranes. It was found that the GAMA grafting degree increases reasonably with the increase of GAMA monomer concentration, and then the increase slows down when the GAMA concentration exceeds 40 g/L. At the same time, a 20–25-min UV irradiation is enough for the grafting polymerization. The water contact angle of the modified membrane decreases from 149 to 64° with the increase of GAMA grafting degree from 0 to 6.18 wt %, which indicates a hydrophilic variation of the membrane surface by the grafting of GAMA. Furthermore, the modified membranes show higher water and protein solution fluxes, lower BSA adsorption, and better flux recovery after cleaning than those of the original PPMM. Platelet adhesion experiment also reveals that a more hemocompatible interface can be obtained between the membrane and the biomolecules.

Introduction

Since it is the surface of a biomedical material which first comes into contact with biological systems (proteins, cells, and microbes) when the materials are used in applications involving cell harvesting, concentration of protein solutions, vascular graft, artificial liver, and sutures, surface properties become more and more important. For example, the adsorption of plasma proteins on the material surface is a crucial step in the thrombus formation, which subsequently could lead to cruro. Furthermore, the biomolecule–material interaction is considered to be basically affected by the physicochemical properties of the material surface, surface free energy, hydrophilicity, and surface morphology.¹ Thus, for biomedical applications, the material surfaces are normally desired to be highly hydrophilic and able to prevent protein adsorption.

Recently, membrane systems have been receiving increased consideration for biomedical applications such as dialysis, plasmapheresis, and oxygenation of blood during cardiac surgery. However, it is well-known that the major obstacle to the extensive use of membrane processes in thera-

peutic treatment is protein fouling of polymeric membrane materials. Protein deposition on the membrane surface can cause instabilities of transport characteristics, and cellular interactions with artificial surfaces are also assumed to be mediated through adsorbed proteins.² Polypropylene, as a promising membrane material, has many desirable properties including very high void volumes, well-controlled porosity, and chemical inertness.³ Therefore, its membranes have been widely used in microfiltration and ultrafiltration processes. Unfortunately, polypropylene microporous membranes (PPMMs) are poor in biocompatibility and nonwettability due to the absence of polar functional groups, which limit their potential application in aqueous solution separation and biomedical usage. In this regard, surface modification is expected to bring desired changes in hydrophilicity and biocompatibility to PPMMs without losing much inherent character.

As we know, adsorption and permeation properties of porous membranes can be changed by the addition of polymeric layers onto their active surface.⁴ For instance, a hydrophilic surface coating on a porous membrane is

* To whom correspondence should be addressed. Fax: ++ 86 571 8795 1773. E-mail: xuzk@ipsm.zju.edu.cn.

[†] Zhejiang University.

[‡] Zhejiang University of Technology.

[§] Universität Duisburg-Essen.

(1) Gupta, B.; Anjum, N. *Adv. Polym. Sci.* **2003**, *162*, 35–61.

(2) Deppisch, R.; Storr, M.; Buck, R.; Gohl, H. *Sep. Pur. Technol.* **1998**, *14*, 241–245.

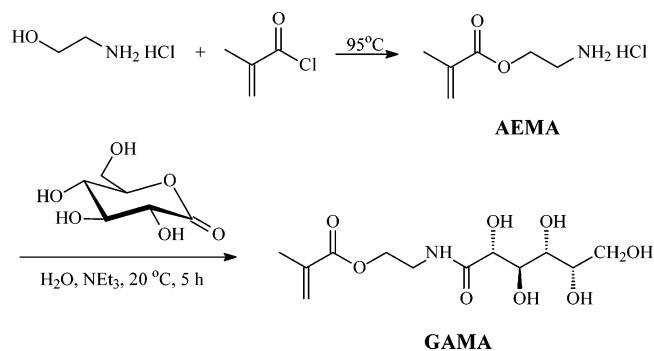
(3) (a) Xu, Z.-K.; Wang, J. L.; Shen, L. Q.; Men, D. F.; Xu, Y. Y. *J. Membr. Sci.* **2002**, *196*, 221–229. (b) Xu, Z.-K.; Dai, Q.-W.; Liu, Z.-M.; Kou, R.-Q. *J. Membr. Sci.* **2003**, *214*, 71–81. (c) Liu, Z.-M.; Xu, Z.-K.; Wang, J.-Q.; Wu, J.; Fu, J.-J. *Eur. Polym. J.* **2004**, *40*, 2077–2087. (d) Liu, Z.-M.; Xu, Z.-K.; Wan, L.-S.; Wu, J.; Ulbricht, M. *J. Membr. Sci.* **2005**, *249*, 21–31.

(4) Zeman, L. J. *J. Membr. Sci.* **1983**, *15*, 213–230.

expected to reduce protein binding and increasing flux. Therefore, one feasible way is to treat the surface of PPMs with appropriate polymerizable monomers and achieve a more compatible interface with organisms. There are quite different covalent and chemical modification methods such as γ -ray irradiation, plasma, and ion beam sputtering. These techniques all involve certain treatment of the surface to create active sites. The activated surface is then contacted with polymerizable monomer in suitable conditions so that the monomer is grafted onto the surface and desirable properties are introduced. However, grafting polymerization induced by γ -ray irradiation or plasma process always results in undesired homopolymer and wastes the starting monomers.³ Furthermore, we expect that the membrane surface should be modified without substantially changing the membrane bulk properties. Taking these into consideration, UV radiation may be the most appropriate and versatile method for us due to several features: low cost of operation, mild reaction conditions, high surface-selectivity, and property alteration of the material surface with facile control of the chemistry.⁵ UV radiation has already been used to modify polymeric materials and a number of studies have been carried out by using photoinitiators^{6–8} or specially synthesized molecules with reactive end groups.^{9,10} As far as we are able to judge, for the surface modification of PPMs, photoinitiator strategy is more convenient and was conducted in this work.

Glycopolymers, in a narrower sense, refer to a kind of synthetic polymers containing sugar moieties. These polymers have been noted in the past decade because of their various functions including excellent biocompatibility and specific protein recognition. Many efforts have been made in the synthesis of sugar-containing monomers and their polymers as reviewed by Wang et al.¹¹ and Ladmiral et al.¹² Therefore, these polymers are expected to display complex functionalities, similar to those of natural glycoconjugates, which might be able to mimic, or even exceed, their performance in specific applications.¹³ Much research has been focused on hydrogels,^{14,15} cell culture substrates,¹⁶ artificial organs,¹⁷ lectin recognition materials,^{18–20} and drug

Scheme 1. Schematic Representation for the Synthesis of D-Gluconamidoethyl Methacrylate



delivery systems.²¹ Also, these polymers are potential surface modifiers for the development of interfacial properties to meet the requirements of biomedical uses. However, few works have been concerned with membrane surface modification by the graft polymerization of the sugar-containing monomer. In our previous study of this series,²² α -allyl glucoside (AG) was synthesized and grafted on a PPM by plasma treatment and some promising results were obtained. Subsequently, lipase immobilization on this modified surface was also achieved.²³ In contrast, vinyl sugars with an open-chain structure were more efficient in improving the hydrophilicity of the polymeric material surface than those with cyclic ones.²⁴ So, herein, a linear sugar was linked to a vinyl group through an amide linkage to produce a novel monomer D-gluconamidoethyl methacrylate (GAMA) (Scheme 1). Then, this monomer was grafted onto PPMs by UV-initiated polymerization to improve the surface hydrophilicity and hemocompatibility.

Experimental Section

Materials. PPMs (purchased from Membrana GmbH, Germany) were prepared by a thermally induced phase separation (TIPS) method with an average pore size of 0.20 μm and a relatively high porosity about 80%. All the membranes used in this study were cut into rotundity with a diameter of 3.95 cm (area = 12.25 cm^2). Before surface modification, the membranes were washed with acetone for 0.5 h to remove any impurities adsorbed on the surfaces, dried in a vacuum oven in 40 $^{\circ}\text{C}$ for 1 h, and then stored in a desiccator. Methacryloyl chloride was a commercial product and was purified by distillation. Ethanolamine, benzophenone, heptane, and D-gluconolactone were analytical grade and were used without further purification. The water used in all synthesis and measurements was deionized.

Synthesis of Ethanolamine Hydrochloride. A 37% (w/w) hydrochloric acid solution (71 mL, 0.875 mol) was added over a period of 2 h to a rapidly stirred mixture of ethanolamine (53 mL,

- (5) Ma, H.; Bowman, C. N.; Davis, R. H. *J. Membr. Sci.* **2000**, *173*, 191–200.
- (6) Richey, T.; Iwata, H.; Oowaki, H.; Uchida, E.; Matsuda, S.; Ikada, Y. *Biomaterials* **2000**, *21*, 1057–1065.
- (7) Ulbricht, M.; Richau, K.; Kamusewitz, H. *Colloids Surf. A* **1998**, *138*, 353–366.
- (8) Kita, H.; Inada, T.; Tanaka, K.; Okamoto, K. *J. Membr. Sci.* **1994**, *87*, 139–147.
- (9) Thom, V.; Altankov, G.; Groth, T.; Jankova, K.; Jonsson, G.; Ulbricht, M. *Langmuir* **2000**, *16*, 2756–2765.
- (10) Taniguchi, M.; Pieracci, J.; Samsonoff, W. A.; Belfort, G. *Chem. Mater.* **2003**, *15*, 3805–3812.
- (11) Wang, Q.; Dordick, J. S.; Linhardt, R. J. *Chem. Mater.* **2002**, *14*, 3232–3244.
- (12) Ladmiral, V.; Melia, E.; Haddleton, D. M. *Eur. Polym. J.* **2004**, *40*, 431–449.
- (13) Albertin, L.; Kohlert, C.; Stenzel, M.; John, L.; Foster, R.; Davis, T. P. *Biomacromolecules* **2004**, *5*, 255–260.
- (14) Chen, X. M.; Dordick, S. J.; David, G. *Macromolecules* **1995**, *28*, 6014–6019.
- (15) Zhou, W. J.; Kurth, M. J.; Hsieh, Y. L.; Krochta, J. M. *J. Polym. Sci., Part A: Polym. Chem.* **1999**, *37*, 1393–1402.
- (16) Bahulekar, R.; Tokiwa, T.; Kano, J.; Matsumura, T.; Kojima, I.; Kodama, M. *Carbohydr. Polym.* **1998**, *37*, 71–78.
- (17) Karamuk, E.; Mayer, J.; Wintermantel, E.; Akaike, T.; Ohashi, Y.; Andrade, A.; Muller, J.; Nose, Y. *Artif. Organs* **1999**, *23*, 881–884.

- (18) García-Oteiza, M. C.; Sánchez-Chaves, M.; Arranz, F. *Macromol. Chem. Phys.* **1997**, *198*, 2237–2247.
- (19) Kobayashi, K.; Tsuchida, A.; Usui, T.; Akaike, T. *Macromolecules* **1997**, *30*, 2016–2020.
- (20) Goldstein, I. J.; Hollerman, C. E.; Smith, E. E. *Biochemistry* **1965**, *4*, 876–883.
- (21) Okahata, Y.; Nakamura, G.; Noguchi, H. *J. Chem. Soc., Perkin Trans. 2* **1987**, 1317–1322.
- (22) Kou, R. Q.; Xu, Z. K.; Deng, H. T.; Liu, Z. M.; Seta, P.; Xu, Y. Y. *Langmuir* **2003**, *19*, 6869–6875.
- (23) Deng, H. T.; Xu, Z. K.; Wu, J.; Ye, P.; Liu, Z. M.; Seta, P. *J. Mol. Catal. B: Enzymol.* **2004**, *28*, 95–100.
- (24) Okada, M. *Prog. Polym. Sci.* **2001**, *26*, 67–104.

0.875 mol) and water (100 mL) at 90 °C. After being stirred for further 1 h at 105–110 °C, the mixture was allowed to cool to room temperature. This solution was then concentrated under vacuum and precipitated into 300 mL of anhydrous ether. The white precipitate was filtered off, washed several times with anhydrous ether, and dried under vacuum at 60 °C with a yield of nearly 95%.

Synthesis of 2-Aminoethyl Methacrylate (AEMA). Ethanolamine hydrochloride (65.0 g, 0.67 mol) and hydroquinone (0.50 g) were mixed together into a four-necked round-bottomed flask fitted with a condenser. The mixture was then heated to around 95 °C under argon atmosphere. With vigorous stirring, methacryloyl chloride (100.0 mL, 0.96 mol) was added slowly into the mixture of the molten salt over 1 h. This reaction mixture was then stirred for further 0.5 h at this temperature and cooled to 60 °C. After that, ethyl acetate (400 mL) was added to precipitate a yellow solid. The precipitate was washed with ethyl acetate and recovered by filtration. The crude product was recrystallized with a 7:3 (v/v) ethyl acetate/2-propanol solution three times to give pure white AEMA powder in its hydrochloride salt form. The yield was 80% (w/w). Calcd. for $C_6H_{12}O_2NCl$: C, 43.50; H, 7.25; O, 19.34; N, 8.46; Cl, 21.45. Found: C, 41.36; H, 7.13; O, 20.01; N, 8.58; Cl, 22.92.

Synthesis of D-Gluconamidoethyl Methacrylate (GAMA). D-Gluconolactone (10.0 g, 56.2 mmol), 2-aminoethyl methacrylate hydrochloride (16.0 g, 96.6 mmol), and triethylamine (13.0 mL) were dissolved in water (100 mL) and the mixture was stirred for 5 h at 20 °C. The reaction solution was then concentrated under vacuum and precipitated into excess 2-propanol. White precipitate of GAMA was obtained. The crude product was washed several times with 2-propanol, and dried under vacuum. The yield was 45%. Calcd. for $C_{12}H_{21}O_8N$: C, 46.91; H, 6.84; O, 41.69; N, 4.56. Found: C, 45.67; H, 6.96; O, 42.80; N, 4.57. 1H NMR spectra of AEMA and GAMA were recorded on a nuclear magnetic resonance spectrometer (Advance DMX500, Bruker) in D_2O solutions at 25 °C with TMS as internal standard.

Surface Modification of PPMMs. GAMA was dissolved in water to prepare a series solution with different monomer concentration. PPMM was dipped into 10 mL of photo-initiator solution (benzophenone in heptane, 1.82 g/L) for 60 min, and then dried in air for 30 min. The dried membrane was then washed with acetone and quickly wiped with filter paper. The membrane with pores still wetted by acetone was immediately fixed between two filter papers (No. 593, Schleicher & Schuell) and immersed into 10 mL of monomer solution in a Petri dish. Then, UV irradiation was done for a predetermined time under argon gas environment. Finally, the membrane was washed with water using a vibrator. After drying in a vacuum oven at 40 °C to constant weight, the grafting degrees, D_g (wt %) and D_a ($\mu g/cm^2$), were calculated by the following equations:

$$D_g = \frac{W_1 - W_0}{W_0}$$

$$D_a = \frac{W_1 - W_0}{A_m}$$

where W_0 is the mass of the nascent membrane and W_1 is the mass of the membrane after modification and drying. A_m represents the area of the membrane. All the results were the average of three parallel experiments.

Surface Characterization and Properties Measurements. To investigate the varieties in surface chemical structure and morphology before and after the modification and to confirm the grafting, surface characterization techniques were used (attenuated total reflectance Fourier transform infrared spectroscopy (FT-IR/ATR),

X-ray photoelectron spectroscopy (XPS), and scanning electron microscopy (SEM)).

FT-IR/ATR measurement was carried out on a Vector 22 FT-IR (Bruker Optics, Switzerland) equipped with an ATR cell (KRS-5 crystal, 45°). Sixteen scans were taken for each spectrum at a resolution of 2 cm^{-1} . XPS measurements of the original and grafted membranes were performed on a PHI 5000c XPS spectrometer (Perkin-Elmer Instruments). Al K α radiation (1486.6 eV) was used as photon source. By using the lowest BE component present in superficial layer, the energy scale of the spectrometer was calibrated. No radiation damage was observed during the data collection time. SEM images were taken on a Cambridge S-260 scanning microscope.

Water Contact Angle Measurement. An OCA20 contact angle system (Dataphysics, Germany) was used for the determination of air/water contact angles at room temperature. Static contact angle was measured by sessile drop method as follows. First, a water drop ($\sim 5\text{ }\mu\text{L}$) was lowered onto the membrane surface from a needle tip. Then, the images of the droplet were recorded in equal time intervals (10 s) for 120 s. Contact angles were determined from these images with calculation software. Advancing angles were measured by adding $5\text{ }\mu\text{L}$ of water to the stationary droplet. Receding angles were measured by removing $5\text{ }\mu\text{L}$ water from the droplet. All results were an average of at least five measurements.

Permeation Properties. Nitrogen gas flux was measured on a gas flux measurement system (GTL-D, China). In a constant pressure, the time of a certain volume of nitrogen gas permeated through the membrane was recorded and the flux (J_g) was calculated as follows:

$$J_g = \frac{V}{PA_t}$$

where V , P , A , and t are the gas volume, pressure, membrane area, and time, respectively.

The water/protein solution flux permeability of the membranes was examined using a permeation cell under constant pressure. A round-shaped membrane was installed into the cell and the pressure in the cell was maintained at 0.1 MPa with nitrogen gas. Thus, pure water was forced to permeate through the membrane, and the flux was recorded (J_w). After that, a 1 g/L BSA phosphate-buffered saline solution (PBS, 19.1008 g of Na_2HPO_4 and 1.8145 g of KH_2PO_4 in 1 L of buffer solution) was forced to permeate through the membrane at the same pressure and the flux was recorded as J_p . To confirm the water flux recovery property of these BSA-permeated membranes, pure water flux was measured (J_R) after cleaning by vibrating in a 0.1 M NaOH solution for 2 h and washing with pure water three times. The relative flux reduction (RFR) and the flux recovery ratio (FRR) were calculated as follows:

$$\text{RFR (\%)} = \left(1 - \frac{J_p}{J_w}\right) \times 100$$

$$\text{FRR (\%)} = \left(\frac{J_R}{J_w}\right) \times 100$$

Adhesion of Blood Platelets. Human platelet-rich plasma (PRP) used in this study was prepared from human fresh blood centrifuged at 1000 rpm for 10 min. The membrane was cut into $1 \times 1\text{ cm}$ pieces and placed in a tissue culture plate. Then, $20\text{ }\mu\text{L}$ of fresh PRP was dropped on the center of the membrane and was allowed to remain at 37 °C for 30 min. After the membrane was rinsed with a PBS (pH = 7.4) solution, the platelets adhered to the membrane were preserved with 2.5 wt % glutaraldehyde in PBS for 30 min. Finally, the sample membrane was washed several times

with PBS, and dehydrated with a series of ethanol/water mixtures (30, 40, 50, 60, 70, 80, 90, 100 vol% ethanol; 30 min in each mixture). The surface of the membrane was observed with a Field Emission SEM (SIRION, FEI) after a gold-sputtering treatment.

Results and Discussion

Monomer Synthesis. The whole process for the monomer synthesis is depicted in Scheme 1. The original synthesis methods of AEMA and GAMA can be found elsewhere.^{25,26} Some changes were made in our strategy. AEMA was synthesized in hydrochloride form to protect the amino group and to reduce the rearrangement reaction.²⁷ Triethylamine was essential for the further reaction of AEMA·HCl with gluconolactone and to prevent the side reaction. High yield (about 80%) was obtained in a short reaction time (1.5 h) for AEMA synthesis. Instead of methanol, water was used as solvent in GAMA synthesis because of the poor solubility of gluconolactone in methanol at room temperature. 2-Propanol was used to precipitate GAMA because the excess AEMA and any rearrangement product can be removed in this selective precipitation process. Characterization of AEMA and GAMA by ¹H NMR in D₂O (Figure 1 a and b) and element analysis confirmed their high purity.

Graft Polymerization of GAMA on PPMs. Figure 2 a and b show the effect of GAMA concentration on the grafting degree (D_g and D_a). As can be seen, the monomer concentration has profound influence on the grafting degree. D_g and D_a increase with the increase of GAMA concentration. However, it can also be observed that the grafting degree increases rapidly with the increase of GAMA concentration from 0 to 40 g/L and then slows down when the monomer concentration exceeds 40 g/L. In our experiments, the membranes were dipped into benzophenone solution for 60 min, and then the solvent was evaporated in air. In this case, the photo-initiator was adsorbed onto the membrane surface. Therefore, with the increase of monomer concentration, the active sites on the membrane surface have more chances to react with GAMA monomer and lead to higher grafting degree accordingly. However, within the same UV radiation time (25 min), the amount of active sites that could be generated on the membrane surface are approximately definite despite the GAMA concentration. For this reason, the grafting degree cannot increase limitlessly. Moreover, at higher monomer concentration, extensive homopolymerization proceeded and consumed much more monomer than that of lower concentration cases. All these cause the slowing down of the grafting degree increase when monomer concentration exceeds a certain value (40 g/L).

The effect of UV radiation time on GAMA grafting degree is shown in Figure 3. In this experiment, 20 g/L and 60 g/L GAMA concentrations were used. In the high monomer concentration case, it can be seen that the grafting degree (D_g) increases obviously with the UV irradiation time at first and then maintains almost a constant when the radiation time

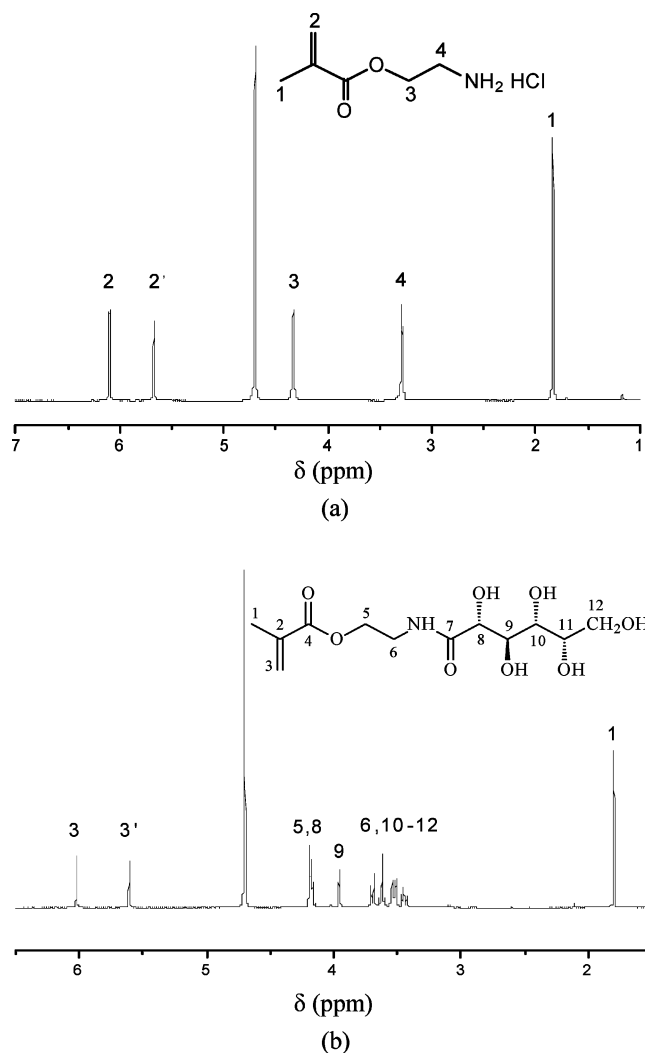


Figure 1. Assigned ¹H NMR spectra for the synthesized 2-aminoethyl methacrylate hydrochloride (a) and D-gluconamidoethyl methacrylate (b).

exceeds 20 min. This phenomenon owes to the fact that with the increase of the UV radiation time, more active sites were produced and more monomers were grafted onto the membrane surface. Whereas, all the PPMs were dipped into the photo-initiator solution for the same interval (60 min) and the adsorbed photo initiator was approximately definite. Consequently, the active sites on the membrane surface cannot increase infinitely, 20–25 min is enough and also ultimate for the membrane surface activation. However, when the monomer concentration is low (20 g/L), the effect of the UV irradiation time on the grafting degree is diminished. That is, the grafting degree increases slightly at first and soon reaches a constant at irradiation time of 15 min. This result can be ascribed to the fact that the monomers are consumed in the first 15 min. Thus, increased UV irradiation time only increases active sites on the membrane surface and no grafting will occur after 15 min.

Chemical and Morphological Changes of the Membrane Surface. Figure 4 is the FT-IR/ATR spectra of the nascent and GAMA-grafted PPMs. The modified membranes show an absorption at 1730 cm⁻¹ which can be attributed to the carbonyl groups in ester bond. Absorptions at 1652 and 1543 cm⁻¹ belong to the amide I and amide II, respectively. An additional broad absorption at 3300 cm⁻¹

(25) Artursson, P.; Brown, L.; Dix, J.; Goddard, P.; Petrak, K. *J. Polym. Sci., Part A: Polym. Chem.* **1990**, *28*, 2651–2663.

(26) Narain, R.; Armes, S. P. *Biomacromolecules* **2003**, *4*, 1746–1758.

(27) Smith, D. A.; Cunningham, R. H.; Coulter, B. *J. Polym. Sci., Part A: Polym. Chem.* **1970**, *8*, 783–784.

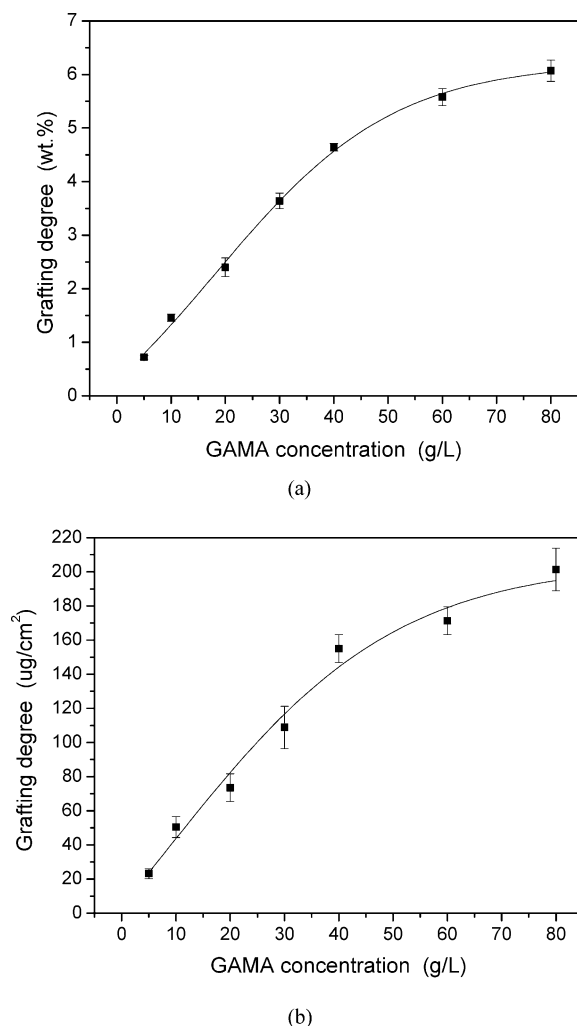


Figure 2. Effect of GAMA concentration on the grafting degrees: (a) D_g ; (b) D_a .

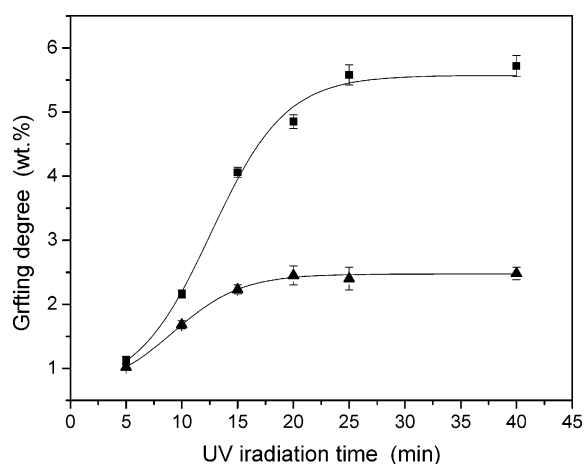


Figure 3. Effect of UV irradiation time on the grafting degree (GAMA concentration: ▲, 20 g/L; ■, 60 g/L).

due to N–H and OH stretching vibration can also be seen at the grafted membranes. The FT-IR spectra indicate clearly the diagnostic absorptions of GAMA and suggest the grafting of GAMA.

For more evidence of the modification, XPS was also employed to confirm the grafting of GAMA. Figure 5 shows the XPS spectra of the nascent and GAMA-grafted membranes. For the nascent PPMMs, there is a major emission

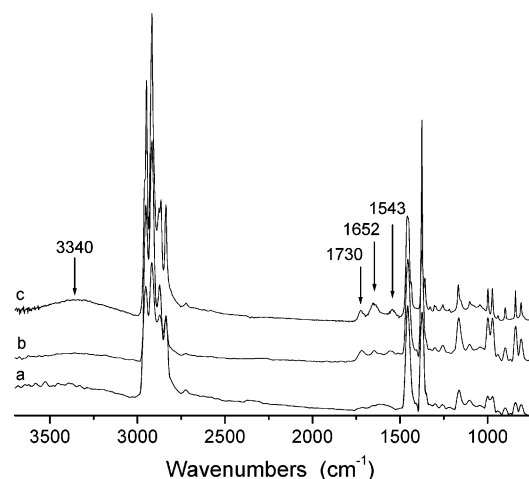


Figure 4. IR spectra of the PPMMs: (a) nascent PPMM; (b) 1.25 wt % GAMA-grafted PPMM; (c) 4.73 wt % GAMA-grafted PPMM.

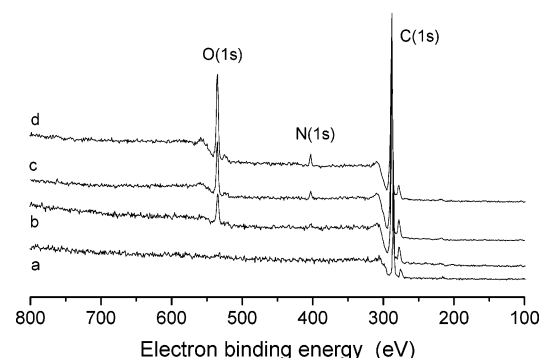


Figure 5. XPS spectra of the nascent and modified PPMMs: (a)–(d) 0, 1.25, 4.73, and 6.28 wt % GAMA-grafted PPMMs, respectively.

peak at 287.4 eV corresponding to the binding energy of C (1s). However, for the GAMA-modified membranes as shown in Figure 5b–d, two additional emission peaks can be observed. These two peaks are at 402.8 eV binding energy for N (1s) and 535.0 eV binding energy for O (1s). Moreover, the intensities of these two peaks increase with the grafting degree of GAMA.

In addition to chemical changes of the membrane surface, we should also consider the surface morphology of the modified PPMMs. For this purpose, SEM pictures of membrane surfaces with different grafting degree were taken. Figure 6 shows the typical images. As can be seen from Figure 6a, the nascent PPMM used in this study shows relatively very high porosity and small pore size. Figure 6 b–d illustrate that the membrane surface was covered by grafted GAMA chains gradually and the porosity decreased, evidently with the increase of the grafting degree from 0 to 6.28 wt %. In the 5000 \times images (b'–d'), we can clearly see that with the increase of GAMA grafting degree, the membrane pores were plugged.

Hydrophilicity of the Membrane Surface. Hydrophilicity is one of the most important factors of the membrane surface and much attention has been paid to it.^{28,29} Commonly, contact angle measurements are the most convenient way to assess changes in the wetting characteristics of the membrane

(28) Steen, M. L.; Jordan, A. C.; Fisher, E. R. *J. Membr. Sci.* **2002**, *204*, 341–357.

(29) Wavhal, D. S.; Fisher, E. R. *Langmuir* **2003**, *19*, 79–85.

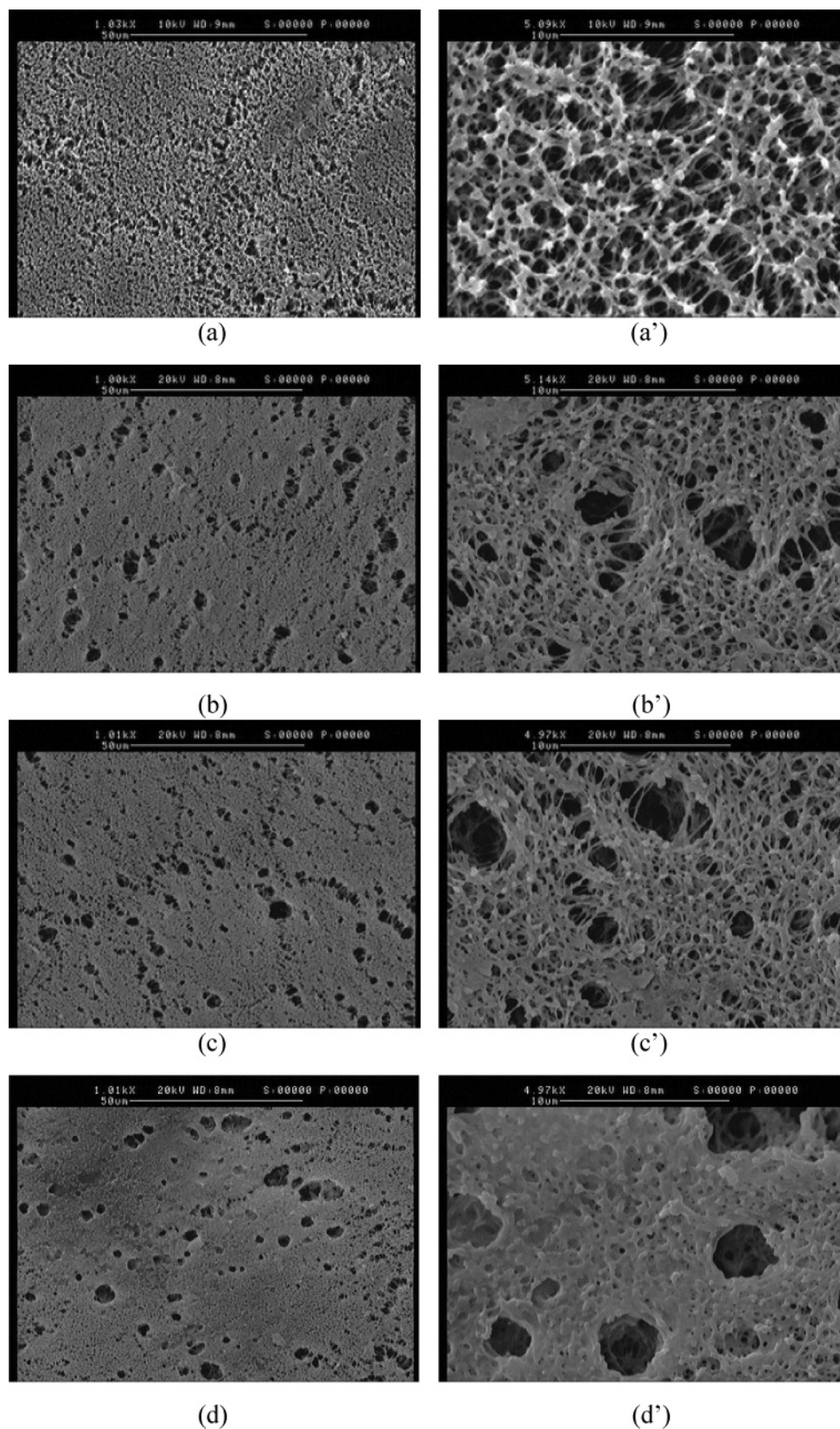


Figure 6. SEM images of the nascent and modified PPMs: (a)–(d) 0, 2.58, 4.72, and 6.28 wt % GAMA-grafted PPMs, respectively (left 1000 \times , right 5000 \times).

surface. Figure 7 is a comparison between the static and dynamic contact angles. It was found that the static, advancing, and receding contact angles decrease greatly with the increase of GAMA grafting degree. The static contact angle decreases evidently from about 149 to 64° with the

increase of GAMA grafting degree from 0 to 6.18 wt %. This decreasing of the contact angle indicates that a highly hydrophilic surface can be obtained by grafting GAMA onto the membrane. This can be ascribed to the contribution of hydroxyl groups in GAMA moieties. Contact angle of the

Table 1. Permeation and Antifouling Properties of the Studied PPMMs

membrane	J_W (kg/m ² ·h)	J_P (kg/m ² ·h)	J_R (kg/m ² ·h)	RFR (%)	FRR (%)
ethanol-wetted	340 ± 7	93 ± 22	219 ± 22	73	64
2.23 wt % GAMA-grafted	466 ± 26	187 ± 24	390 ± 26	60	84
3.50 wt % GAMA-grafted	608 ± 21	348 ± 37	488 ± 38	57	80
4.58 wt % GAMA-grafted	729 ± 14	452 ± 38	646 ± 30	38	89
5.47 wt % GAMA-grafted	762 ± 22	434 ± 32	658 ± 33	57	86
6.03 wt % GAMA-grafted	764 ± 28	452 ± 25	649 ± 35	59	85

nascent PPMM used in this study is higher than general ones (about 100–120°) because of relatively high surface porosity, or, accordingly, roughness.³⁰ In addition, with the increase of grafting degree the discrepancy in static contact angle (or advancing contact angle) and receding contact angle was enlarged. This could also be ascribed to the increase of hydrophilicity due to the grafting of sugar moieties. Figure 8 shows the time dependence of contact angle on the PPMMs

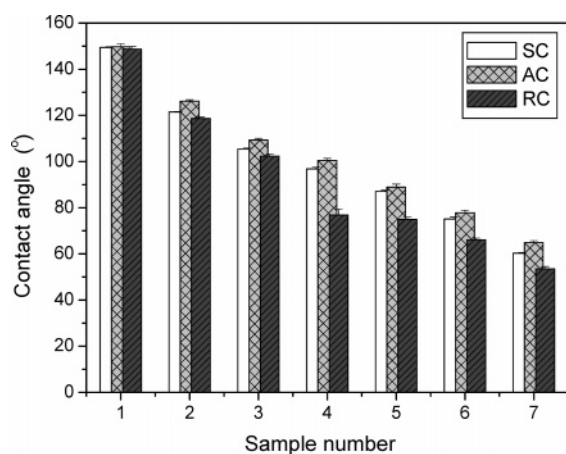


Figure 7. Comparison of advancing contact angle (AC), receding contact angle (RC), and static contact angle (SC) on the nascent and modified PPMMs: (1)–(7) 0, 1.52, 2.58, 3.79, 4.72, 5.76, and 6.28 wt % GAMA-grafted PPMMs, respectively.

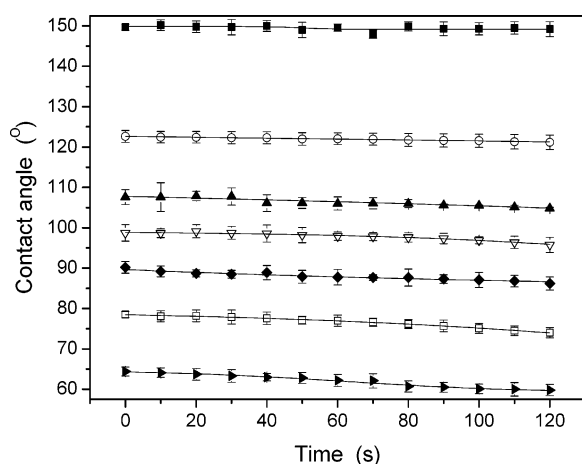


Figure 8. Time dependence of water contact angle on the nascent and GAMA-modified PPMMs: (■) 0, (○) 1.52, (▲) 2.58, (▽) 3.79, (◆) 4.72, (□) 5.76, and (▲) 6.28 wt % GAMA-grafted PPMMs.

with various GAMA grafting degrees. Each sample was measured for 2 min and data was collected every 10 s to construct the curves in this figure. It was found that the contact angles almost remain stable when the grafting degree is relatively low. However, in higher grafting degree cases the contact angles reduce gradually within the measurement

time. This decay of contact angles has been expressed as diffusion-controlled reaction by some researchers, and some models have also been established to correlate the change of contact angle during the aging processes.^{31,32} In our experience, the more hydrophilic the sample surface is, the more evident the decrease of contact angle in the measurement time.

Permeation and Antifouling Properties. Pure water and nitrogen gas permeation measurements were carried out to characterize the permeation properties of the modified membranes. The water permeability of the nascent and ethanol-wetted membranes were also measured and compared with those of modified ones. Figure 9 shows the results

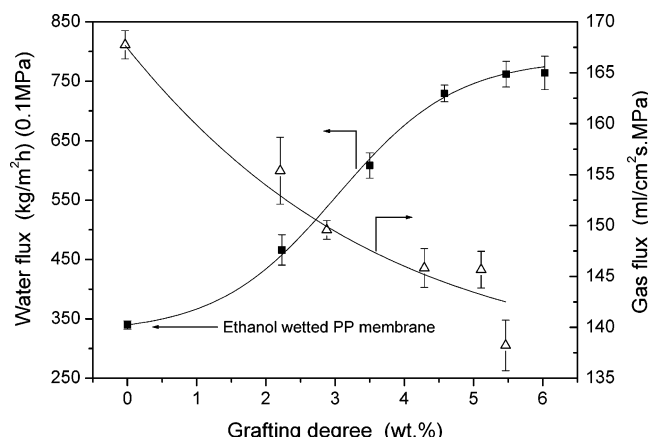


Figure 9. Permeation properties of the nascent and GAMA-grafted PPMMs: (■) pure water flux, and (□) nitrogen gas flux.

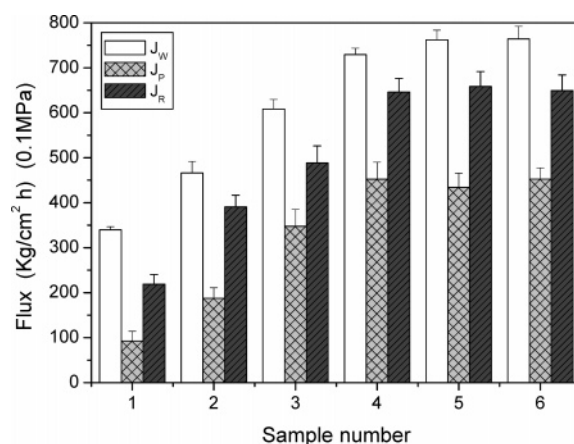


Figure 10. Permeation fluxes of pure water and BSA solution through the nascent and GAMA-grafted PPMMs: (1)–(6) 0, 2.23, 3.50, 4.58, 5.47, and 6.03 wt % GAMA-grafted PPMMs, respectively.

obtained by matching the water and gas flux curves for the original and modified membranes. The nascent membrane

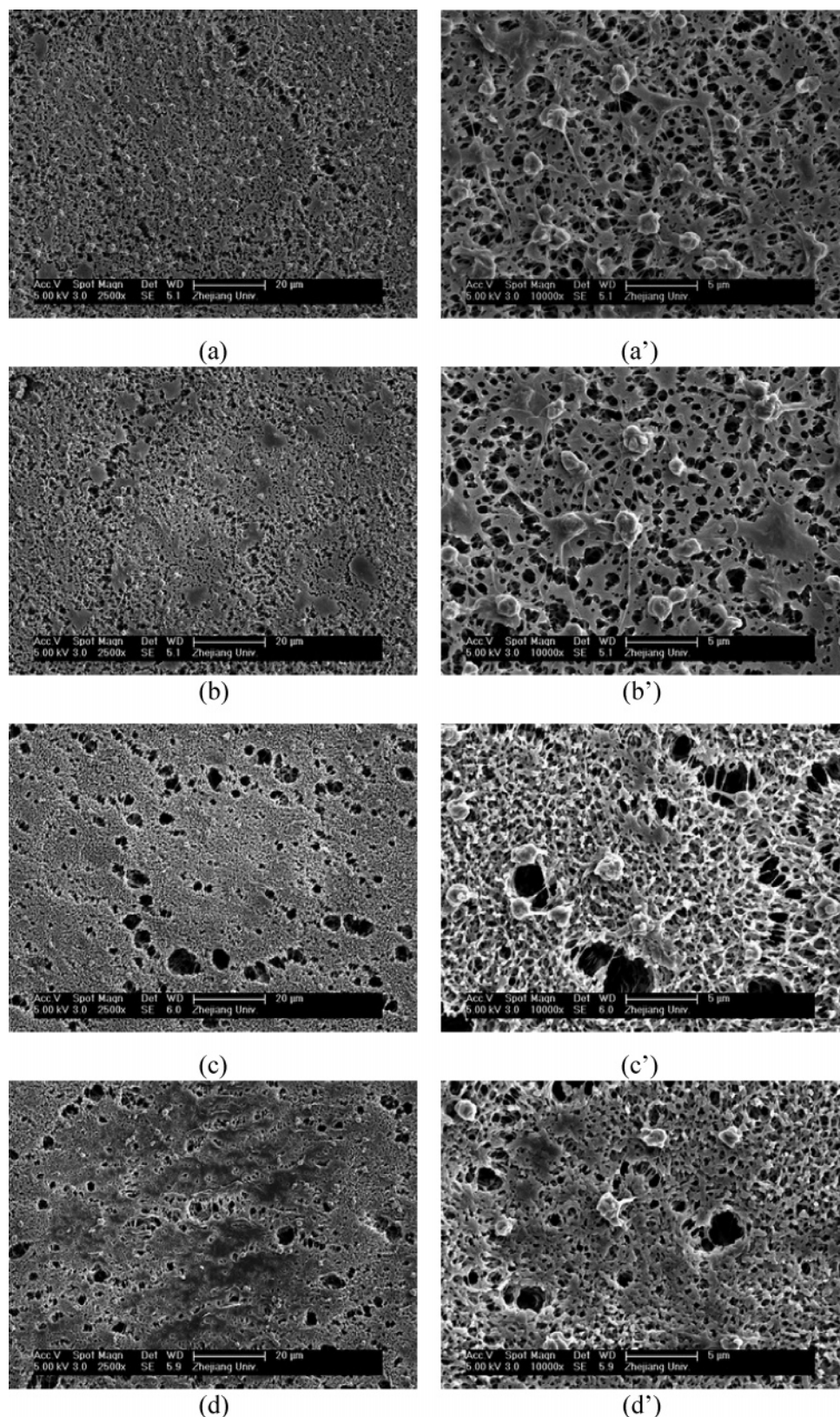


Figure 11. Scanning electron micrographs of adhered platelets on the nascent and modified PPMMs: (a)–(d) 0, 1.52, 4.72, and 6.28 wt % GAMA-grafted PPMMs, respectively (left 2500 \times , right 10 000 \times).

cannot let water flow across in our case. The flux of ethanol-wetted membrane is $340 \pm 7 \text{ kg/m}^2\cdot\text{h}$. It can be seen that, with the increase of GAMA grafting degree from 2.23 to 6.03 wt %, the water flux increases from 466 ± 26 to $764 \pm 28 \text{ kg/m}^2\cdot\text{h}$. Moreover, the GAMA-grafted membranes exhibit a more stable water permeability than that of ethanol-

wetted ones which declines obviously over time. In contrast, the gas flux reduces with the grafting progression. This is due to the pore blocking mentioned above according to the SEM images. These reverse phenomena in water and gas permeability seem to be ambivalent and confusing. However, in this study, pore size and surface hydrophilicity are the

two parameters which affect water flux most. As shown in Figure 9, when the grafting degree is low, the surface hydrophilicity is the dominant factor and the water flux enhances with the increase of grafting degree accordingly despite pore blocking. However, pore blocking becomes the leading factor at higher grafting degree and causes the decline of the water flux. Nevertheless, for the gas flux, the pore size and porosity are both reduced by the grafting and the gas flux decreases when the pores are plugged even slightly at lower grafting degree.

For various, especially biomedical, applications of polypropylene membranes, protein adsorption is the initial problem to conquer and is expected to be reduced as much as possible. Questions remain, yet, about the mechanism of membrane protein fouling and there are quite different theories.^{33–35} Belford et al.³⁶ concluded that major contribution of the protein fouling is from protein deposition during the dynamic and convective flow conditions. Thus, a dynamic protein solution permeation process was conducted in this study and BSA was used as a model protein to examine the anti-fouling properties of the original and modified membranes. It was found from Figure 10 and Table 1 that the flux decreases with the permeation of BSA solution due to the deposition of proteins. The ethanol-wetted nascent membrane shows the largest loss of flux within the measurement time, which suggests that a large amount of BSA protein had deposited on the membrane surface. However, the flux reduction can be restrained by GAMA grafting and indicates that the GAMA polymer layer is able to prevent the adsorption of BSA effectively. Moreover, the recovery flux increases significantly with the increase of grafting degree, and even at lower grafting degree a relatively high flux recovery ratio (>80%) was achieved. However, when the grafting degree increases to some extent the RFR tends to decrease. This result may be attributed to the fouling mechanism, that is, where the fouling does occur. When the grafting degree was relatively low, small protein particles permeated through the membrane pores expediently. Fouling only took place on the membrane surface by protein aggregates deposition. On the other hand, as the grafting degree went along, membrane pores were blocked gradually and small protein particles accumulated in the pores. Thus, fouling took place both on the membrane surface and in the membrane pores. Moreover, proteins in the membrane pores cannot be washed off by the lye. For this reason, the RFR shows a decrease at high grafting degree. All these results demonstrate that the anti-fouling properties of the PPMMs can be improved greatly by the grafting of GAMA.

Hemocompatibility of the Membrane Surface. The hemocompatibility of the GAMA-grafted membranes was evaluated by platelet adhesion experiments.³⁷ It can be seen from Figure 11 a and a' that platelets adhere seriously on the nascent PPMM. However, the platelets adhesion on the membrane surface can be reduced greatly by the GAMA grafting (see Figure 11b–d). The restraint of platelet adhesion might be ascribed to the striking hydrophilicity of polyGAMA chains. Besides the number of adhered platelets, the morphology of the platelet is one of the indexes expressing the degree of the surface hemocompatibility.³⁸ As can be seen from Figure 11a'–d', for the nascent and lower grafting degree (1.52 wt %) membranes, the adhered platelets show a large size as well as the tendency of aggregation and hair-like filaments can also be found. These indicate the activation of the platelets by the surface. In the cases of higher GAMA grafting degree (4.72 and 6.28 wt %), the adhered platelets remain almost spherical shape, which means that the surface did not activate the platelets. Taking these aspects into consideration, the number and the shape of the adhered platelets, we can conclude that grafting GAMA onto the membrane surface is an efficient and achievable way to improve the hemocompatibility of the PPMM.

Conclusions

A novel sugar-containing monomer GAMA was grafted onto the surfaces of PPMMs by an UV-induced photografting process (BP as photo initiator). The grafting degree can be adjusted by both monomer concentration and UV irradiation time. The chemical and morphological changes of the modified membrane surfaces can be confirmed by FT-IR/ATR, XPS, and SEM. The decrease of the water contact angles and the increase of the pure water flux for the modified PPMMs indicate the improvement of the surface hydrophilicity by the grafting of GAMA. Results in BSA solution permeation and platelet adhesion experiments imply strongly that a considerable enhancement of biocompatibility can be achieved.

Acknowledgment. Financial support from the National Nature Science Foundation of China (Grant 20474054) and the National Basic Research Program of China (Grant 2003CB15705) are gratefully acknowledged. Z.-K.X. thanks both Deutsche Forschungsgemeinschaft (DFG) and the Education Ministry of China for financial support for the visit of a Chinese guest scientist to Germany.

CM048012X

- (33) Kim, K. J.; Fane, A. G.; Fell, C. J. D.; Joy, D. C. *J. Membr. Sci.* **1992**, *68*, 79–91.
- (34) Kelly, S. T.; Opong, W. S.; Zydney, A. L. *J. Membr. Sci.* **1993**, *40*, 175–187.
- (35) Tracey, E. M.; Davis, R. H. *J. Colloid Interface Sci.* **1994**, *167*, 104–116.
- (36) Belford, G.; Davis, R. H.; Zydney, A. L. *J. Membr. Sci.* **1994**, *96*, 1–58.

- (37) (a) Nie, F.-Q.; Xu, Z.-K.; Huang, X.-J.; Ye, P.; Wu, J. *Langmuir* **2003**, *19*, 9889–9895. (b) Xu, Z.-K.; Dai, Q.-W.; Wu, J.; Huang, X.-J.; Yang Q. *Langmuir* **2004**, *20*, 1481–1488.
- (38) Tanaka, M.; Mochizuki, A.; Ishii, N.; Motomura, T.; Hatakeyama, T. *Biomacromolecules* **2002**, *3*, 36–41.